Supplementary Fig. 1

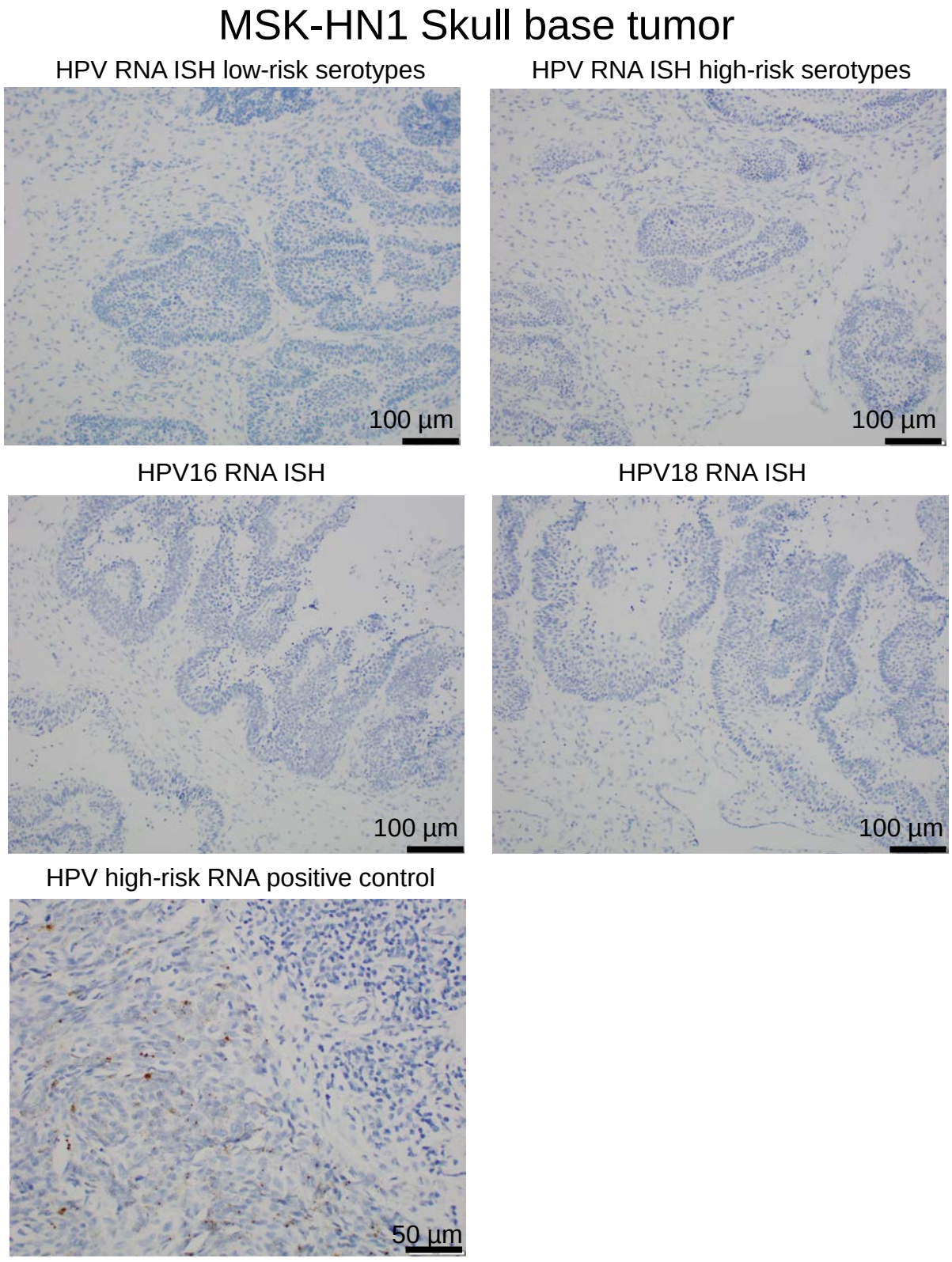

HPV low-risk strains: 6, 11, 40, 43, 44, 54, 69, 70, 71, 74
HPV high-risk strains: 16, 18, 26, 31, 33, 35, 39, 45, 51, 52, 53, 56, 58, 59, 66, 68, 73, 82

Supplementary Fig. 1 – RNA *in situ* hybridization (ISH) for human papilloma virus (HPV). RNA *in situ* hybridization (ISH) for human papilloma virus (HPV) low-risk and high-risk serotypes, as well as HPV16 and HPV18 strains, indicates that the skull base tumor from Patient MSK-HN1 was not associated with HPV. RNA ISH was performed once with appropriate controls in a Clinical Laboratory Improvement Amendments certified clinical laboratory.

Supplementary Fig. 2

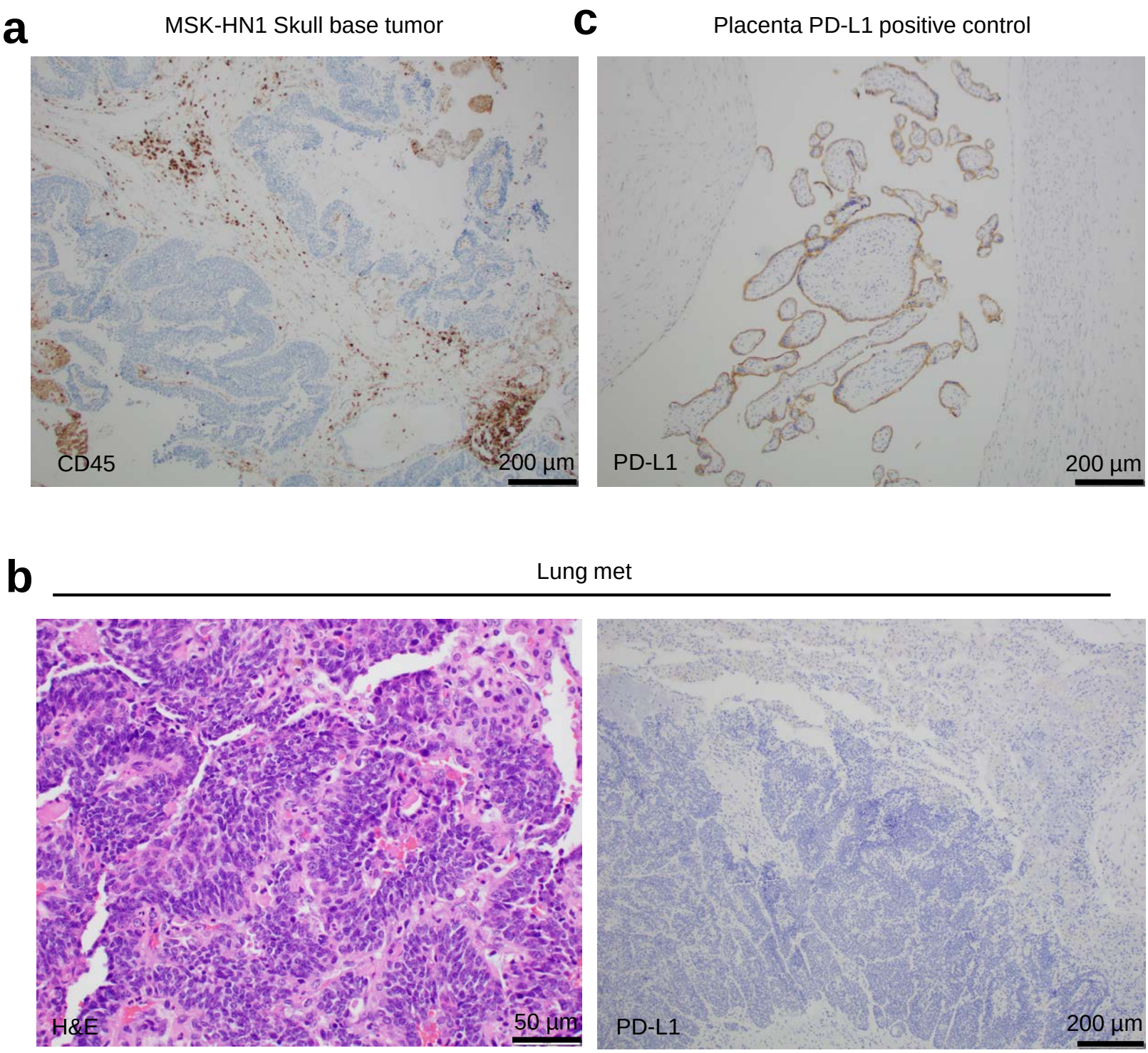

Supplementary Fig. 2 – Immunohistochemistry staining of Patient MSK-HN1 samples. **a.** Immunohistochemistry staining for CD45 in the primary skull base tumor of Patient MSK-HN1 revealed a modest level of immune infiltration prior to any treatment. **b.** An additional tissue section of lung metastasis demonstrated no PD-L1 staining, with **c.** PD-L1 positive control. IHC staining was performed at least twice with appropriate controls in a Clinical Laboratory Improvement Amendments certified clinical laboratory.

Supplementary Fig. 3

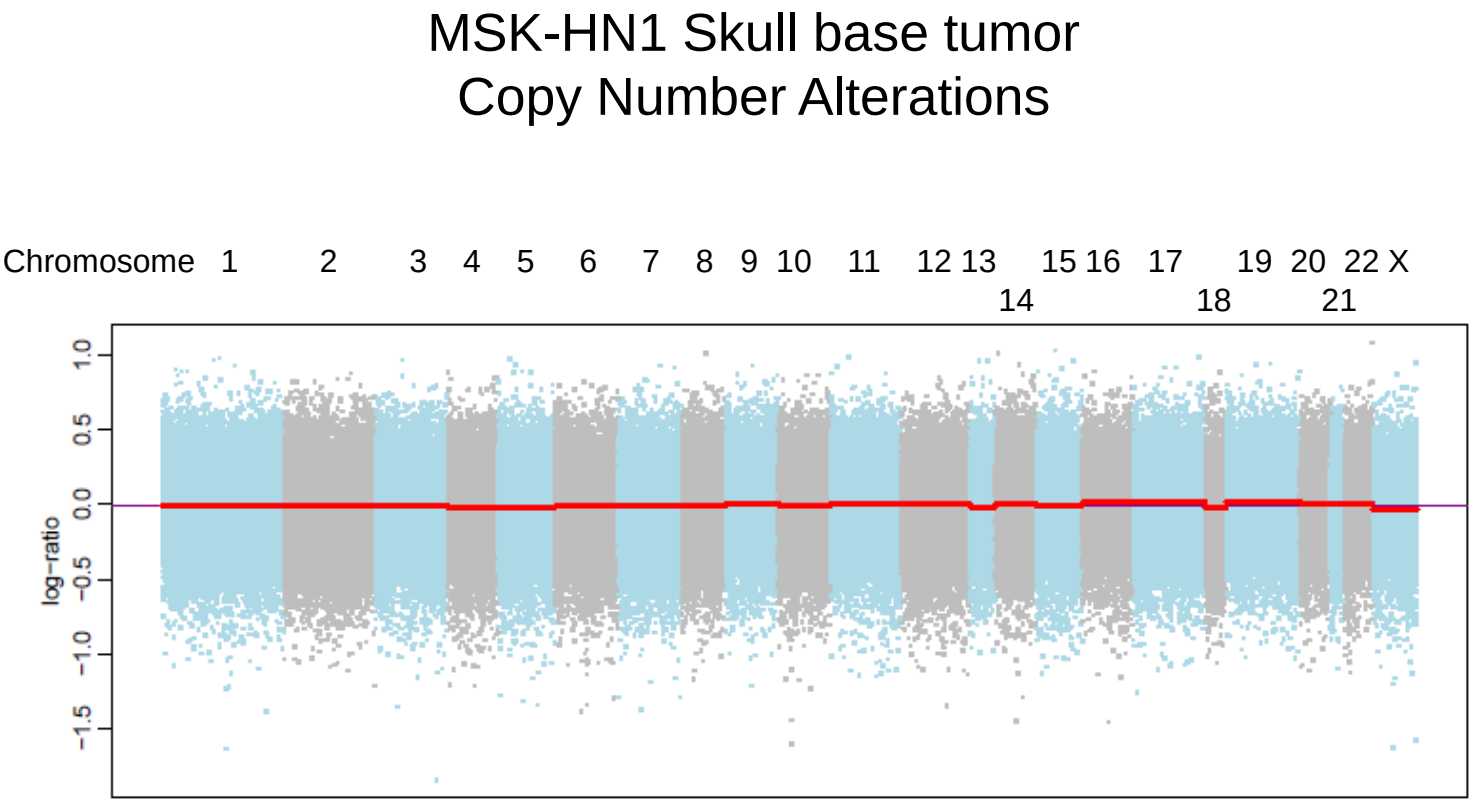

Supplementary Fig. 3 – FACETS analysis of Patient MSK-HN1's skull base tumor reveals no significant copy number variations. The red line is the segmentation line showing copy number by chromosomal region, and the y-axis represents log copy number ratio, where 0 represents the diploid genome.

Supplementary Fig. 4

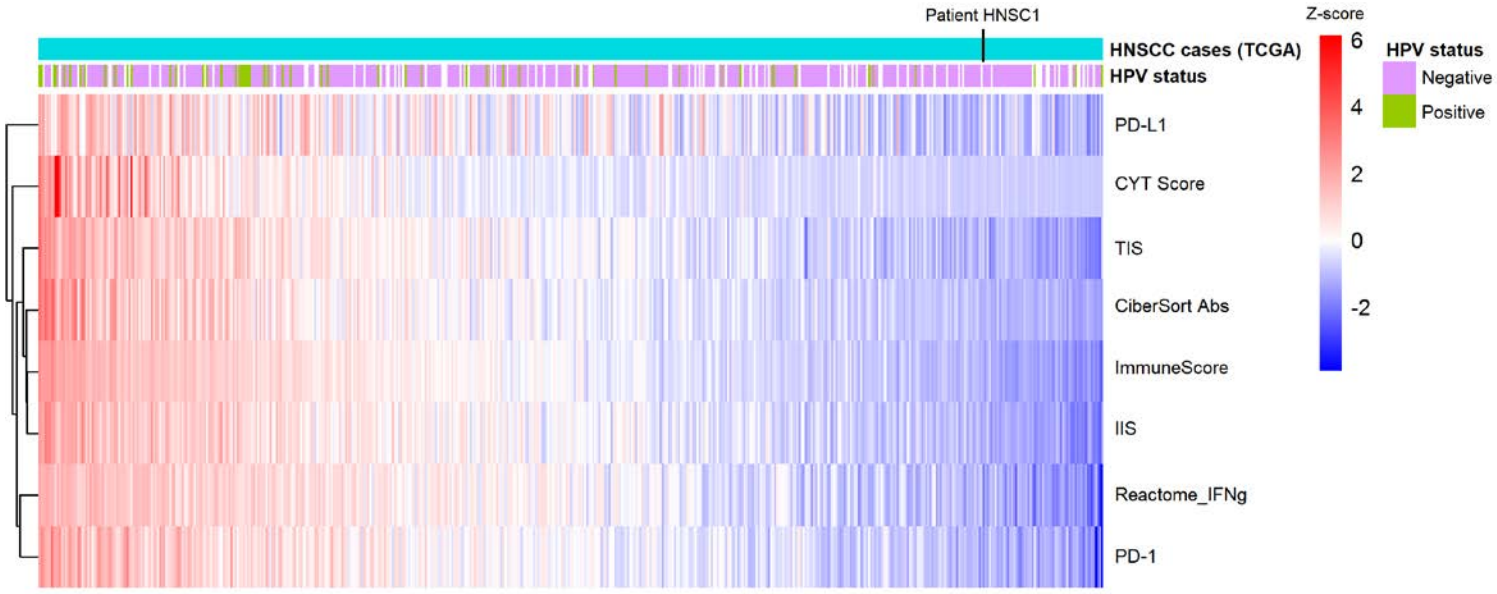

Supplementary Fig. 4 – Comparison of Patient MSK-HN1's skull base tumor's immune characteristics and tumors in the TCGA HNSCC dataset. The MSK-HN1 tumor is relatively lowly immune infiltrated compared to other HNSCC tumors, as measured by Immune Infiltration Score (IIS), T cell Infiltration Score (TIS), ESTIMATE ImmuneScore, CiberSort Absolute Score, CYT Score, and interferon-γ signaling (Reactome.org). The MSK-HN1 tumor had very low PD-L1 and PD-1 expression, consistent with **Fig. 1d**.

Supplementary Fig. 5

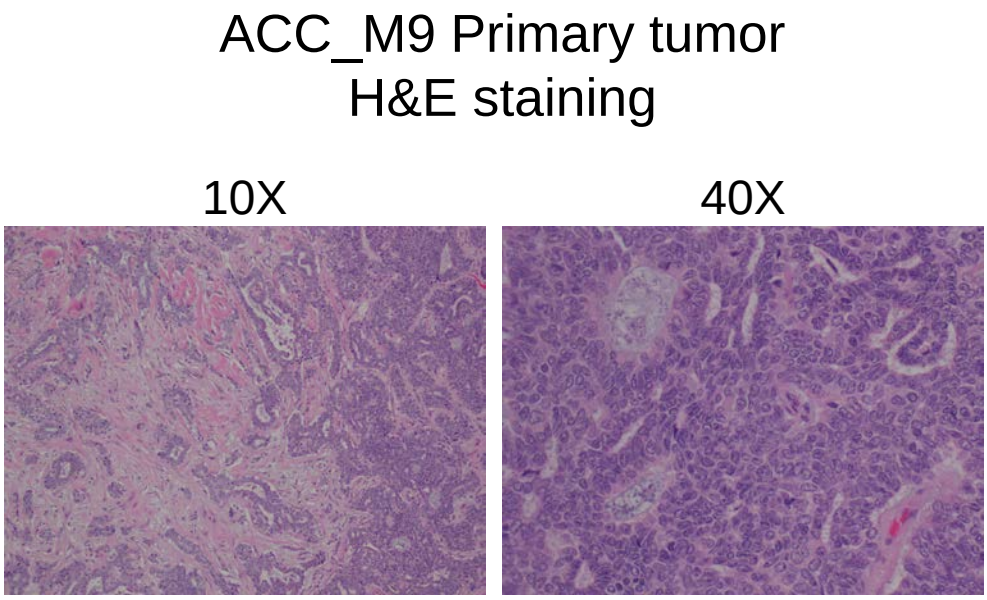

Supplementary Fig. 5 – H&E staining of formalin-fixed paraffin-embedded (FFPE) slides from Patient ACC_M9 tumor acquired prior to treatment. The adenoid cystic carcinoma histology was confirmed (by N.K.). Staining was performed once as part of clinical care in a Clinical Laboratory Improvement Amendments certified clinical laboratory.

Supplementary Fig. 6

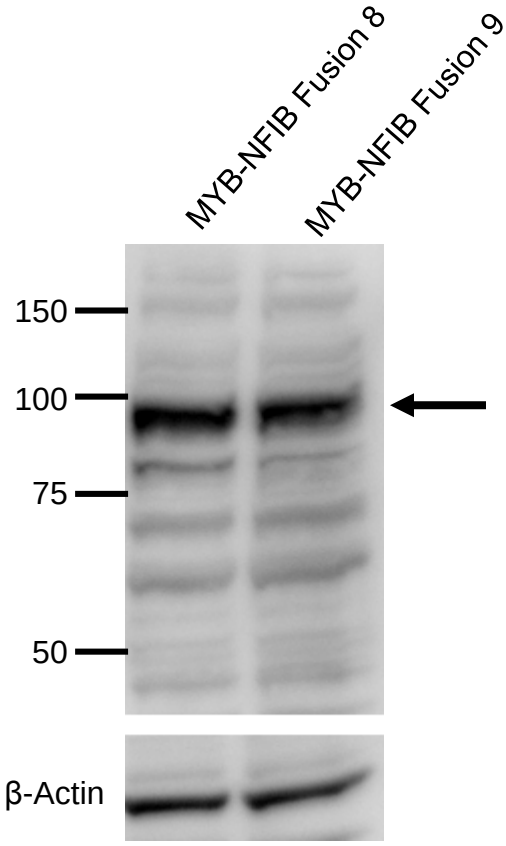

Supplementary Fig. 6 – Immunoblot confirming the expression of MYB-NFIB fusion constructs. HEK293 cells were transfected with pcRNA6SL-MYB-NFIB fusion plasmids and cell lysates were collected after 48 hr. The lysates were blotted and probed with anti-MYB antibody. Data are representative of two independent experiments.

Supplementary Fig. 7

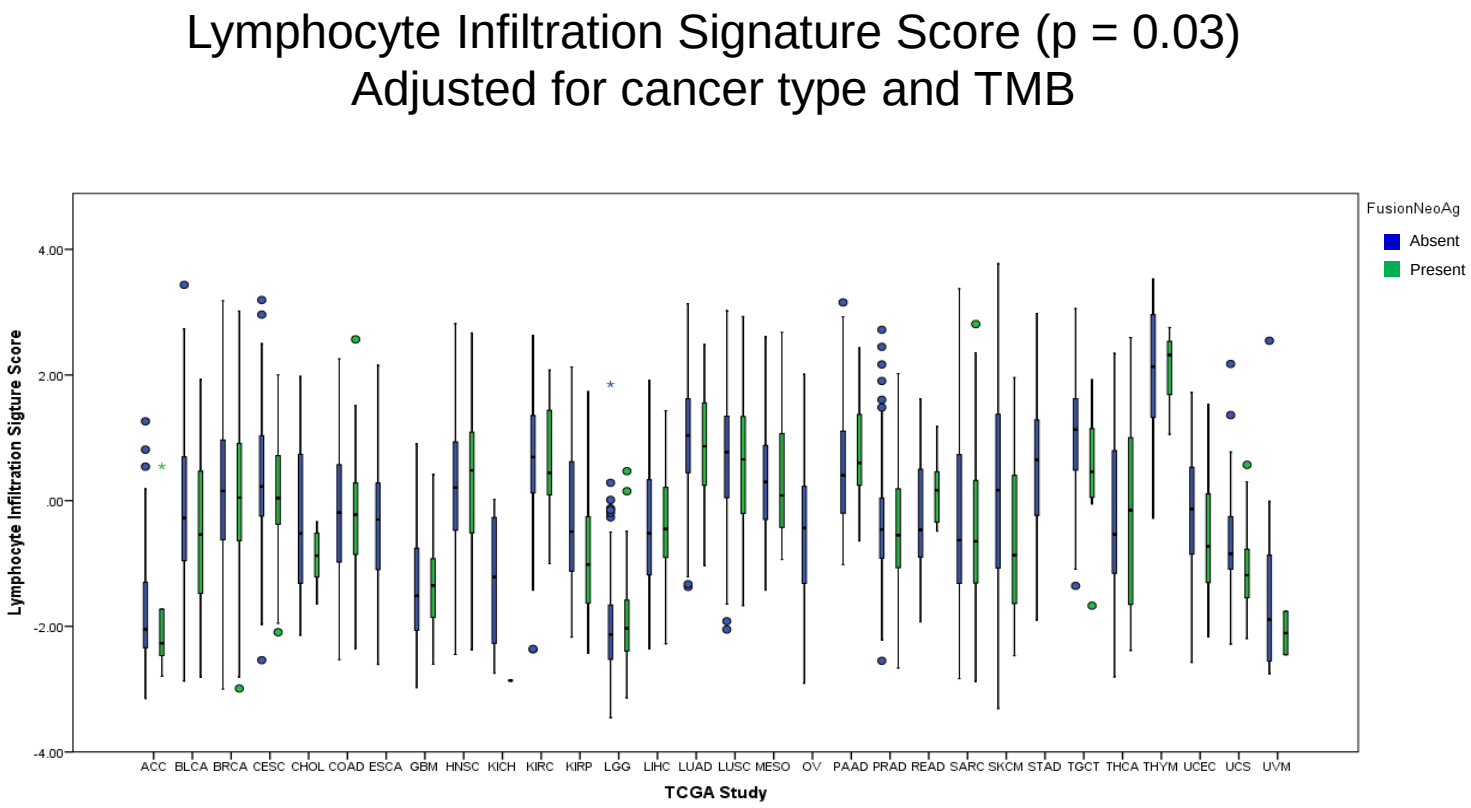

Supplementary Fig. 7 – Solid tumors with gene fusion products that are predicted to bind patient-specific HLAs (“Fusion NeoAg” present) have lower leukocyte fraction and lymphocyte infiltration signature than solid tumors with a fusion gene present but without a predicted neoantigen that binds HLA (“Fusion NeoAg” = absent). Multi-variate linear regression analysis was performed on 5,825 samples across 30 cancer types from TCGA data adjusting for cancer type and mutational load. The boxes represent the median and interquartile range, the whiskers represent 1.5x the interquartile range, and dots indicate values beyond 1.5 IQR.

Supplementary Fig. 8

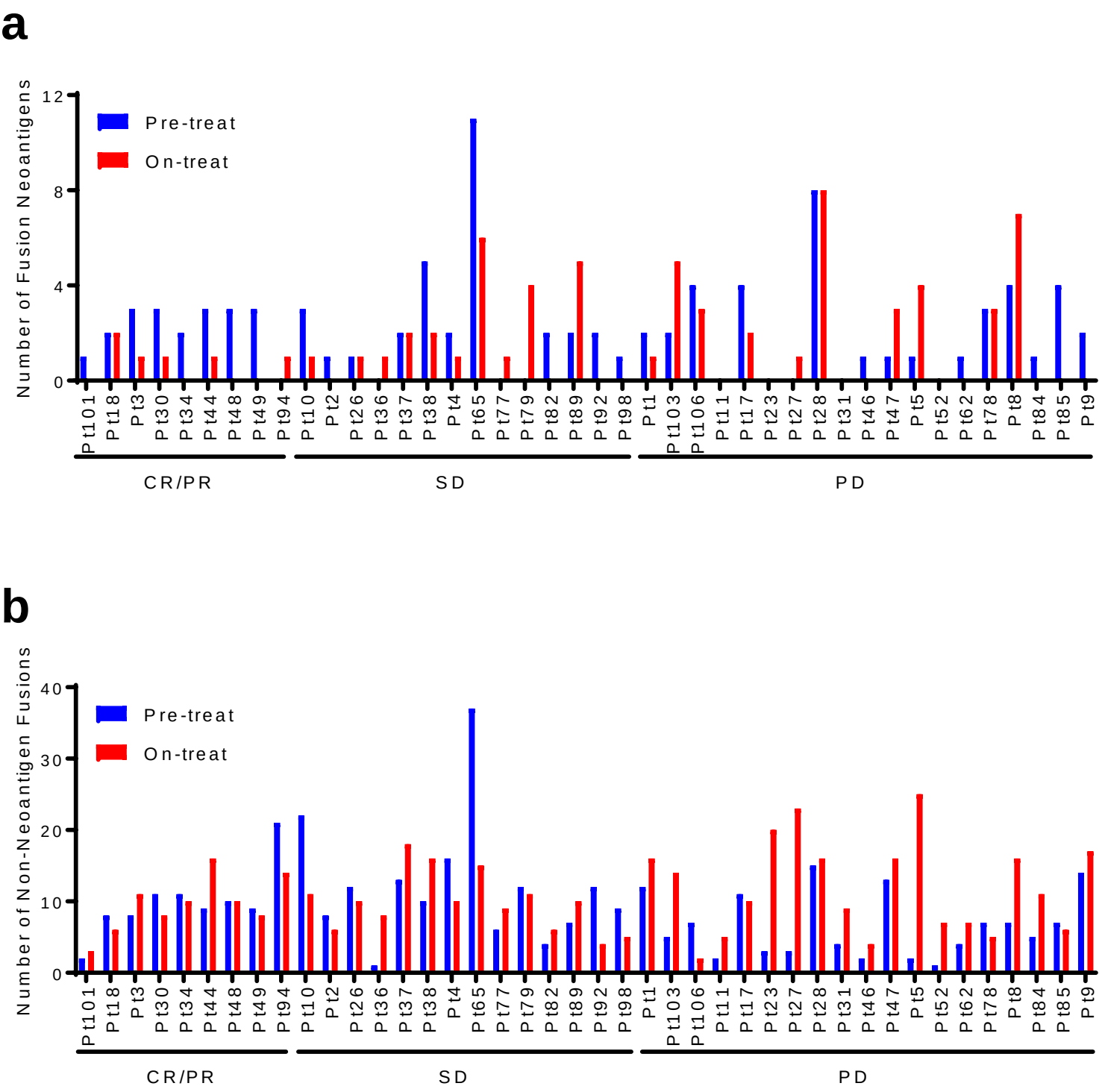

Supplementary Fig. 8 – **a.** Change in fusion neoantigens detected in melanomas treated with anti-PD-1 therapy from pre-therapy and on-therapy timepoints. **b.** Change in non-neoantigen fusions detected in melanomas treated with anti-PD-1 therapy from pre-therapy and on-therapy timepoints.

Supplementary Table 1 – Genetic alterations in Patient HNSC1. The gene fusion DEK-AFF2 and the reciprocal fusion AFF2-DEK are shown with the chromosomal coordinates of the breakpoints. SNVs (missense mutations) are also shown with their respective chromosomal coordinates.

Fusions

	Breakpoint 1	**Breakpoint 2**
DEK-AFF2	Chr 6: 18249882	Chr X: 147891400
AFF2-DEK	Chr X: 147744289	Chr 6: 18237747

SNV (missense mutations)

Gene	**Nucleotide change**	**Amino Acid Change**	**Entrez Gene ID**	**Transcript ID**	**Chromosome**	**Start Position**	**Most common nonsilent mutation reported in COSMIC**
SUV39H2	c.574T>G	p.S192A	79723	NM_001193424.1	10	14939241	R213fs*2 (9 cases, all occurred in clear cell renal cell carcinoma)
MTUS2	c.895G>C	p.A299P	23281	NM_001033602.2	13	29599700	E193K (3 cases in prostate adenocarcinoma, 1 in stomach adenocarcinoma)
PCSK6	c.998G>A	p.R333Q	5046	NM_002570.4	15	101933625	A302V (3 cases); R71Q (3 cases)
COX5A	c.163C>T	p.R55C	9377	NM_004255.3	15	75221511	D81N (3 cases)
NPIPB5	c.1991G>C	p.R664P	440345	NM_001135865.1	16	22546295	P485-A488delPPSA (10 cases, 3 of which are in HNSCC); F616C (5 cases in hematopoietic neoplasms)
LIG1	c.1493A>T	p.E498V	3978	NM_000234.2	19	48638967	D570E (4 cases in serous carcinoma)
ZNF460	c.1067G>A	p.R356Q	10794	NM_006635.3	19	57802976	E127K (4 cases)
OR7D4	c.350T>C	p.V117A	125958	NM_001005191.2	19	9325164	V49I (6 cases)
STAU1	c.345G>C	p.R115S	6780	NM_001322932.1	20	47768284	L181V (5 cases)
OTOP1	c.1793G>C	p.R598P	133060	NM_177998.1	4	4190576	L104_W106delLLW (38 cases, recurrent in HNSCC); L226fs*1 (6 cases, 5 in thyroid cancer)
OTOP1	c.1792C>G	p.R598G	133060	NM_177998.1	4	4190577	
OTOP1	c.1774C>G	p.P592A	133060	NM_177998.1	4	4190595	
DSPP	c.2017G>A	p.D673N	1834	NM_014208.3	4	88535831	Several inframe indels; D673N (6 cases)
COL14A1	c.890C>T	p.A297V	7373	NM_021110.3	8	121215960	R566Q (10 cases, none of which are in HNSCC); L793I (5 cases); T636M (5 cases)

Non-protein coding SNVs

GPRC5B	c.265C>T	None	51704	NM_001304771.1	16	19896652	
DCLK2	c.961+2T>C	None	166614	NM_001040261.4	4	151119257	

Supplementary Table 2 – SNV-derived peptides predicted to bind Patient HNSC1 HLAs. All possible 9-amino acid length peptide combinations that were predicted to bind significantly to patient-specific HLAs are shown (NetMHCpan 4.0, Rank <2%) (left). Since one neoantigen peptide can be predicted to bind to multiple HLAs, we generated a list of unique peptides (right). The mutated amino acid is indicated by a capital letter.

Gene	WT Peptide	MUT Peptide	HLA binder	WT Rank (%)	MUT Rank (%)
COL14A1	lfaigvknA	lfaigvknV	C0401	7.5371	1.7933
COL14A1	vknAdvnel	vknVdvnel	B3801	0.8639	1.0801
COL14A1	faigvknAd	faigvknVd	C1203	1.2	1
COX5A	efdaRwvty	efdaCwvty	A2601	0.6723	1.9058
COX5A	efdaRwvty	efdaCwvty	C0401	0.05	0.015
COX5A	efdaRwvty	efdaCwvty	B3501	2.5	1.2
COX5A	fdaRwvtyf	fdaCwvtyf	A2601	1.3	1.3
COX5A	fdaRwvtyf	fdaCwvtyf	C1203	0.7	0.6
COX5A	fdaRwvtyf	fdaCwvtyf	B3501	2.5	1.3
COX5A	fdaRwvtyf	fdaCwvtyf	C0401	1.2	1.7
LIG1	ktwleEqgm	ktwleVqgm	C1203	3.6738	1.4143
LIG1	twleEqgmi	twleVqgmi	C0401	1.8116	1.3717
LIG1	wleEqgmil	wleVqgmil	C0401	0.2746	0.8927
LIG1	earktwleE	earktwleV	A2601	7	2
LIG1	earktwleE	earktwleV	C1203	13	1.6
LIG1	eEqgmilkq	eVqgmilkq	A2601	16	1.7
LIG1	twleEqgmi	twleVqgmi	C0401	1.8	1.2
LIG1	wleEqgmil	wleVqgmil	B3801	0.5	1.5
LIG1	wleEqgmil	wleVqgmil	C0401	0.175	0.6
MTUS2	Askeipskl	Pskeipskl	C1203	1.3	1.8
MUC4	lHvtspssa	lPvtspssa	B3501	22	0.7
MUC4	tplHvtsps	tplPvtsps	B3501	0.6	0.5
MUC4	tplHvtsps	tplPvtsps	C0401	3.5	1.7
NPIPB5	eRmiisrhl	ePmiisrhl	B3501	10.7657	0.7124
NPIPB5	grfhpeRmi	grfhpePmi	B3801	0.8555	0.5429
NPIPB5	hpeRmiisr	hpePmiisr	B3501	2.9458	1.0847
NPIPB5	rfhpeRmii	rfhpePmii	C0401	0.443	0.1805
NPIPB5	rfhpeRmii	rfhpePmii	C1203	1.8336	1.4276
OR7D4	aVmaydrfv	aAmaydrfv	C1203	1.7773	1.1533
OR7D4	dtfllaVma	dtfllaAma	A2601	2.6329	1.9769
OR7D4	gmdtfllaV	gmdtfllaA	A0201	0.1103	0.4718
OR7D4	laVmaydrf	laAmaydrf	C1203	1.9922	1.4779
OR7D4	laVmaydrf	laAmaydrf	B3501	0.7973	0.5256
OR7D4	tfllaVmay	tfllaAmay	B3501	1.8548	1.5468
OR7D4	tfllaVmay	tfllaAmay	A2601	1.3856	1.6105
OR7D4	aVmaydrfv	aAmaydrfv	C1203	3.5	1.1
OR7D4	mdtfllaVm	mdtfllaAm	B3501	1.7	0.9
OR7D4	tfllaVmay	tfllaAmay	C0401	2.5	1.4
OTOP1	fsifyRmha	fsifyPmha	C1203	2.4647	1.0555
OTOP1	ifyRmhaaa	ifyPmhaaa	C0401	6.1722	1.3124
OTOP1	mpfsifyRm	mpfsifyPm	A2601	0.9093	1.9852
OTOP1	mpfsifyRm	mpfsifyPm	B3501	0.0426	0.0954
OTOP1	sifyRmhaa	sifyPmhaa	A0201	1.4724	1.058
OTOP1	sifyRmhaa	sifyPmhaa	A2601	1.9683	1.2785
OTOP1	sifyRmhaa	sifyPmhaa	C1203	1.5422	1.2836
OTOP1	yRmhaaasl	yPmhaaasl	A2601	5.0155	1.6443
OTOP1	yRmhaaasl	yPmhaaasl	B3501	3.99	0.0175
OTOP1	yRmhaaasl	yPmhaaasl	B3801	0.03	0.9608
OTOP1	yRmhaaasl	yPmhaaasl	C0401	0.6502	0.9436
OTOP1	yRmhaaasl	yPmhaaasl	C1203	0.3364	0.4647
OTOP1	fsifyRmha	fsifyGmha	C1203	2.4647	1.7387
OTOP1	mpfsifyRm	mpfsifyGm	C1203	1.3206	1.6499
OTOP1	mpfsifyRm	mpfsifyGm	B3501	0.0426	0.0703
OTOP1	mpfsifyRm	mpfsifyGm	A2601	0.9093	0.8701
OTOP1	Rmhaaaslf	Gmhaaaslf	C0401	0.6938	1.795
OTOP1	sifyRmhaa	sifyGmhaa	A0201	1.4724	0.615
OTOP1	sifyRmhaa	sifyGmhaa	A2601	1.9683	1.3761
OTOP1	sifyRmhaa	sifyGmhaa	C1203	1.5422	1.1766
OTOP1	yRmhaaasl	yGmhaaasl	C1203	0.3364	0.0714
OTOP1	yRmhaaasl	yGmhaaasl	C0401	0.6502	1.5099
OTOP1	yRmhaaasl	yGmhaaasl	B3501	3.99	1.7778
OTOP1	ivvnlamPf	ivvnlamAf	B3501	1.0456	0.4401
OTOP1	ivvnlamPf	ivvnlamAf	C1203	0.9286	0.2542
OTOP1	ivvnlamPf	ivvnlamAf	A2601	0.8402	0.3307
OTOP1	lamPfsify	lamAfsify	B3501	0.0607	0.1994
OTOP1	lamPfsify	lamAfsify	A2601	0.2469	0.6221
OTOP1	lamPfsify	lamAfsify	C1203	0.0457	0.3645
OTOP1	mPfsifyrm	mAfsifyrm	C1203	1.3206	0.1679
OTOP1	mPfsifyrm	mAfsifyrm	A2601	0.9093	0.4634
OTOP1	mPfsifyrm	mAfsifyrm	B3501	0.0426	0.3217
OTOP1	nlamPfsif	nlamAfsif	A2601	0.6079	0.8682
PCSK6	gRqglgsif	gQqglgsif	B3801	0.6024	0.916
PCSK6	feygikkGr	feygikkQr	C0401	2.5	2
PCSK6	Grqglgsif	Qrqglgsif	B3801	1	0.5
STAU1	gayppRyfy	gayppSyfy	C0401	1.3205	1.0705
STAU1	gayppRyfy	gayppSyfy	A2601	0.3473	0.2725
STAU1	gayppRyfy	gayppSyfy	B3501	0.1777	0.0943
STAU1	gayppRyfy	gayppSyfy	C1203	0.0386	0.0341
STAU1	ggayppRyf	ggayppSyf	C1203	1.5962	1.4309
STAU1	rggayppRy	rggayppSy	C1203	3.4846	1.9164
STAU1	yppRyfypf	yppSyfypf	B3501	0.3753	0.1695
STAU1	yppRyfypf	yppSyfypf	A2601	2.71	1.6
ZNF460	shlkqheRi	shlkqheQi	B3801	0.4039	0.2099
ZNF460	Rihtgekpf	Qihtgekpf	B3501	4	2
ZNF460	shlkqheRi	shlkqheQi	B3801	0.5	0.25

Unique Peptides	
COL14A1	lfaigvknV
COL14A1	vknVdvnel
COL14A1	faigvknVd
COX5A	efdaCwvty
COX5A	fdaCwvtyf
LIG1	ktwleVqgm
LIG1	twleVqgmi
LIG1	wleVqgmil
LIG1	earktwleV
LIG1	eVqgmilkq
MTUS2	Pskeipskl
MUC4	lPvtspssa
MUC4	tplPvtsps
NPIPB5	ePmiisrhl
NPIPB5	grfhpePmi
NPIPB5	hpePmiisr
OR7D4	aAmaydrfv
OR7D4	dtfllaAma
OR7D4	gmdtfllaA
OR7D4	laAmaydrf
OR7D4	tfllaAmay
OR7D4	mdtfllaAm
OTOP1	fsifyPmha
OTOP1	ifyPmhaaa
OTOP1	mpfsifyPm
OTOP1	sifyPmhaa
OTOP1	yPmhaaasl
OTOP1	fsifyGmha
OTOP1	mpfsifyGm
OTOP1	Gmhaaaslf
OTOP1	sifyGmhaa
OTOP1	yGmhaaasl
OTOP1	ivvnlamAf
OTOP1	lamAfsify
OTOP1	mAfsifyrm
OTOP1	nlamAfsif
PCSK6	gQqglgsif
PCSK6	feygikkQr
PCSK6	Qrqglgsif
STAU1	gayppSyfy
STAU1	ggayppSyf
STAU1	rggayppSy
STAU1	yppSyfypf
ZNF460	shlkqheQi
ZNF460	Qihtgekpf

HLA-A*02:01 peptides are highlighted

Supplementary Table 3 – Fusion-derived peptides predicted to bind Patient HNSC1 HLAs. All possible 9-amino acid length peptide combinations surrounding the fusion breakpoints of DEK-AFF2 or AFF2-DEK are listed with the predicted patient-specific HLA binding values (NetMHCpan 4.0).

		HLA-A0201	HLA-A2601	HLA-B3501	HLA-B3801	HLA-C0401	HLA-C1203
Peptide	Fusion	Rank (%)	Rank (%)	Rank (%)	Rank (%)	Rank (%)	Rank (%)
FTILQTSEP	AFF2-DEK	28.3913	15.7193	21.7468	44.4444	42.1379	13.6372
TILQTSEPP	AFF2-DEK	38.5882	61	38.9	68.125	70.625	61.9048
ILQTSEPPK	AFF2-DEK	25.5652	43.1818	42.8571	69.375	19.8059	45.2794
LQTSEPPKK	AFF2-DEK	33.8519	35.2632	38.2	35.72	23.329	35.9632
QTSEPPKKT	AFF2-DEK	43.8	19.9918	42.7143	42.4167	48.3158	24.8581
TSEPPKKTA	AFF2-DEK	40.5	36.5294	16.8542	32.7143	12.8303	13.8082
SEPPKKTAK	AFF2-DEK	49.2857	14.6642	21.3165	30.7111	14.7184	28.6823
EPPKKTAKR	AFF2-DEK	61.7857	10.3687	13.388	63.5	54.726	34.7905
EDKESEEEV	DEK-AFF2	47.625	23.1791	24.549	18.6382	36.2979	57.1721
DKESEEEVS	DEK-AFF2	96.6667	92.5	69.1667	56.6667	89.1667	92.7778
KESEEEVSL	DEK-AFF2	11.0349	13.2667	4.5523	0.7586	5.4378	13.8115
ESEEEVSLP	DEK-AFF2	68	44.6667	41.5	64	78.6842	73.0769
SEEEVSLPS	DEK-AFF2	53.7037	40.0769	21.519	21.4771	44.875	64.6429
EEEVSLPSD	DEK-AFF2	95	85	55.9091	49.5	84.6875	95.8333
EEVSLPSDP	DEK-AFF2	83	71.25	42.7143	32.2	84.0625	95
EVSLPSDPS	DEK-AFF2	55.5263	11.6012	17.5443	54.375	66.7188	51.4021

Peptide with predicted significant binding is highlighted

Peptide in which Patient MSK-HN1 autologous T cells have reactivity towards

Supplementary Table 4 – Primer sequences for cloning the DEK-AFF2 fusion. The cloning strategy is shown with the appropriate primer pairs.

Primer name	Sequence	Comments	Template
DEK-N-term			
DEK-1F	CACACA-GAATTC-ATGTCCGCCTCGGCCCCTGCTGC	PCR with DEK-1F + DEK-2R, digest with EcoRI and BamHI	Patient MSK-HN1 cDNA (from FFPE tumor RNA)
DEK-2R	CACACA-GGATCC-CTCCTCTTCACTTTCTTTATCTTCATC		
DEK-AFF2			
DEK-1F	CACACA-GAATTC-ATGTCCGCCTCGGCCCCTGCTGC	PCR with DEK-1F + DEK-1R, digest with EcoRI and BsmBI	Patient MSK-HN1 cDNA (from FFPE tumor RNA)
DEK-1R	CACACA-CGTCTCC-TTAC-CTCCTCTTCACTTTCTTTATCTTCATC		
AFF2-1F	CACACA-CGTCTCC-GTAAGCCTTCCCAGTGATCCAAG	PCR with AFF2-1F + AFF2-2R, digest with BsmBI and BamHI	Patient MSK-HN1 cDNA (from FFPE tumor RNA)
AFF2-2R	CACACA-GGATCC-AGTGGGCCGTGGACGGGCTTTCTC		

Supplementary Table 5 - TCRβ clone frequencies in patient tissues pre- and on- treatment.

GLIPH group name	CDR3s	CRG_Score	Motifs
CRG-SSPRGNEQF	10	2.01E-13	PRGN(7, 0.001)

Peptide	Frequency				
	IFNγ+ T cells	Pre-treatment tumor	On-therapy PBMCs		
		Mar-16	Mar-17	Jun-17	Jul-18
SSPRGNEQF	2.70%	0	0.00326%	0.0016%	0.0000%
SSPRGDEQF	0.0007%	0	0.0000%	0.0016%	0.00178%

Pre-treatment and on-therapy refer to pembrolizumab treatment

Supplementary Table 7 - Alternative Splicing-derived peptides predicted to bind Patient MSK-HN1 HLAs. Alternative splicing events with high PSI (percentage spliced inclusion; indicating the percentage of transcripts with the event) of 10% or greater are shown. The 9-amino acid length peptide combinations of these alternative splicing events that were predicted to bind significantly to patient-specific HLAs are shown (NetMHCpan 4.0, Rank <2%).

Gene	PSI.median_a	PSI.mean_annc	PSI.sum
MROH2A	0.4689655	0.408817635	0.0535433
OBSCN	0.2368421	0.233711048	0.0027372
MROH2A	0.2222222	0.182825485	0.0173228
ICA1L	0.2195122	0.225402504	0.020362
OC90	0.2028986	0.175438596	0.0200573
EPHB6	0.1612903	0.156895128	0.0096525
MED12L	0.122449	0.080163599	0.0017406
CARD16,CASP1,CASP1P2	0.1142857	0.067523584	0.005165
RP11-274B21.1	0.1044776	0.105315948	0.007014
RBM19	0.1034483	0.104675506	0.0046332

Gene	AS Peptide	HLA binder	Rank (%)
MED12L	QTMPQGYTMY	HLA-A26:01	0.1164
MED12L	QTMPQGYTM	HLA-B35:01	0.2933
MED12L	QTRPFQQTM	HLA-C12:03	0.1609
MROH2A	IAACNLAAL	HLA-B35:01	2.1569
MROH2A	IAACNLAAL	HLA-C12:03	0.3414

Peptide with predicted significant binding is highlighted

Supplementary Table 8 – Predicted binding of MYB-NFIB / NFIB-MYB / MYBL1-NFIB fusion-derived peptides in ACC tumors. INTEGRATE-Neo results combining HLAminer results (HLA typing from RNA-seq data) and identified fusion peptides for binding affinity prediction (NetMHC 4.0) (Column E). During preparation of the manuscript, NetMHCpan 4.0 was released and a comparison of the predicted binding is shown (Column F). In addition, since some HLA sequences are highly homologous, NetMHCpan 4.0-predicted peptide affinities to HLA-A*02:01 are also shown (Column G). A list of unique peptides is provided (right).

Patient	Fusion	Peptide sequence	HLA	HLA Affinity (nM) - NetMHC4	NetMHCpan 4 (% Rank)	NetMHCpan 4 for HLA-A0201 (% Rank)
ACC_M1	NFIB>>MYB	MMYSPICLTQT	HLA-A02:03	414.87	3.7205	5.3193
ACC_M1	MYB>>NFIB	QQVLPSWYL	HLA-A02:02	252.74	1.8534	1.9713
ACC_M1	MYB>>NFIB	QQVLPSWYL	HLA-A02:06	11.91	1.8534	0.4054
ACC_M1	MYB>>NFIB	ELKGQQSWYL	HLA-A02:02	440.89	6.7919	11.4535
ACC_M1	NFIB>>MYB	YSPICLTQFL	HLA-A02:02	419.26	17.3021	24.7792
ACC_M1	MYB>>NFIB	QQLRICDWTM	HLA-A02:06	260.1	6.4577	14.2117
ACC_M9	MYB>>NFIB	TLQFIDSLRI	HLA-A02:02	264.35	2.6228	2.2614
ACC_M9	MYB>>NFIB	LQFIDSLRI	HLA-A02:06	170.89	1.1201	2.9587
ACC_M9	MYB>>NFIB	SLRICDWTM	HLA-A02:16	115.26	5.6458	5.0656
ACC_M9	MYB>>NFIB	LQFIDSSWYL	HLA-A02:01	17.62	1.4432	1.4432
ACC_M9	MYB>>NFIB	LQFIDSSWYL	HLA-A02:02	16.08	1.6007	1.4432
ACC_M9	MYB>>NFIB	LQFIDSSWYL	HLA-A02:03	180.74	4.0551	1.4432
ACC_M9	MYB>>NFIB	LQFIDSSWYL	HLA-A02:06	5.07	0.5295	1.4432
ACC_M9	MYB>>NFIB	FIDSSWYL	HLA-A02:11	188.14	1.0686	1.0378
ACC_M9	MYB>>NFIB	FIDSSWYL	HLA-A02:12	43.41	1.0009	1.0378
ACC_M9	MYB>>NFIB	FIDSSWYL	HLA-A02:16	32.27	1.2373	1.0378
ACC_M9	MYB>>NFIB	QFIDSSWYL	HLA-A02:17	192.27	0.2664	1.3362
ACC_M9	NFIB>>MYB	FLHQQQFL	HLA-A02:02	286.14	1.7123	2.4742
ACC_M9	NFIB>>MYB	FLHQQQFLNT	HLA-A02:03	389.32	4.4795	5.4084
ACC_M9	MYB>>NFIB	SLPFSPSQL	HLA-A02:02	72.74	0.6031	1.4913
ACC_M9	MYB>>NFIB	SLPFSPSQL	HLA-A02:03	27.08	0.6352	1.4913
ACC_M9	MYB>>NFIB	SQLRICDWTM	HLA-A02:06	159.29	4.3985	8.3925
ACC_M9	MYB>>NFIB	SLPFSPSQL	HLA-A02:11	381.8	0.8647	1.4913
ACC_P11	MYB>>NFIB	SLASPLQLRI	HLA-A02:01	421.08	0.894	0.894
ACC_P11	MYB>>NFIB	SLASPLQLRI	HLA-A02:02	17.15	0.5527	0.894
ACC_P11	MYB>>NFIB	SLASPLQLRI	HLA-A02:03	28.72	0.3469	0.894
ACC_P11	MYB>>NFIB	LQLRICDWTM	HLA-A02:06	103.75	9.0628	14.3081
ACC_P11	MYB>>NFIB	SLASPLQSWYL	HLA-A02:01	96.81	0.9213	0.9213
ACC_P11	MYB>>NFIB	SLASPLQSWYL	HLA-A02:02	17.99	0.6348	0.9213
ACC_P11	MYB>>NFIB	LASPLQSWYL	HLA-A02:06	227.85	10.8546	14.1418
ACC_P11	MYB>>NFIB	PLQSWYLG	HLA-A02:11	264.27	83.5714	80
ACC_P11	MYB>>NFIB	SLASPLQPT	HLA-A02:01	358.35	1.4285	1.4285
ACC_P11	MYB>>NFIB	SLASPLQPT	HLA-A02:02	102.89	1.1757	1.4285
ACC_P11	MYB>>NFIB	SLASPLQPT	HLA-A02:03	20.61	0.604	1.4285
ACC_P11	MYB>>NFIB	SLASPLQPT	HLA-A02:06	149.34	1.5454	1.4285
ACC_P11	MYB>>NFIB	SLASPLQPT	HLA-A02:11	21.46	0.8618	1.4285
ACC_P11	MYB>>NFIB	PLQPTQPQA	HLA-A02:16	171.36	8.4943	6.0986
ACC_P13	MYBL1>>NFIB	MQLRICDWTM	HLA-A02:06	45.44	5.866	10.7078
ACC_P13	MYBL1>>NFIB	ISDMQSWYL	HLA-A02:06	319.32	2.1031	3.4677
ACC_P13	MYBL1>>NFIB	DMQSWYLG	HLA-A02:11	196.4	76.6667	78
ACC_P13	MYBL1>>NFIB	IVLRICDWTM	HLA-A02:06	424.18	11.5055	12.5907
ACC_P13	MYBL1>>NFIB	VLRICDWTM	HLA-A02:11	364.85	6.5228	6.1286
ACC_P13	MYBL1>>NFIB	VLRICDWTM	HLA-A02:16	264.36	7.1899	6.1286
ACC_P14	MYB>>NFIB	SLASPLQSWYL	HLA-A02:02	17.99	0.6348	0.9213
ACC_P14	MYB>>NFIB	LASPLQSWYL	HLA-A02:06	227.85	10.8546	14.1418
ACC_P14	MYB>>NFIB	PLQSWYLG	HLA-A02:11	264.27	83.5714	80
ACC_P15	MYBL1>>NFIB	SLRICDWTM	HLA-A02:16	115.26	5.6458	5.0656
ACC_P15	MYBL1>>NFIB	KRIPSSWYL	HLA-A02:06	254.21	1.0669	2.4367
ACC_M18	MYB>>NFIB	SLASPLQLRI	HLA-A02:01	421.08	0.894	0.894
ACC_M18	MYB>>NFIB	LQLRICDWTM	HLA-A02:06	103.75	9.0628	14.3081

HLA-A*02:01 peptides are highlighted
Peptide in which Patient ACC_M9 autologous T cells have reactivity towards

Unique MYB-NFIB / NFIB-MYB / MYBL1-NFIB peptides predicted to bind HLA-A*02

Sequence	Fusion
QQVLPSWYL	MYB-NFIB
ELKGQQSWYL	MYB-NFIB
QQLRICDWTM	MYB-NFIB
TLQFIDSLRI	MYB-NFIB
LQFIDSLRI	MYB-NFIB
LQFIDSSWYL	MYB-NFIB
FIDSSWYL	MYB-NFIB
QFIDSSWYL	MYB-NFIB
SLPFSPSQL	MYB-NFIB
SQLRICDWTM	MYB-NFIB
SLASPLQLRI	MYB-NFIB
LQLRICDWTM	MYB-NFIB
SLASPLQSWYL	MYB-NFIB
LASPLQSWYL	MYB-NFIB
PLQSWYLG	MYB-NFIB
SLASPLQPT	MYB-NFIB
PLQPTQPQA	MYB-NFIB
ETLQFIDSLR	MYB-NFIB
AETLQFIDSL	MYB-NFIB
LQFIDSSWY	MYB-NFIB
AETLQFIDSSW	MYB-NFIB
SLPFSPSQLR	MYB-NFIB
LPFSPSQL	MYB-NFIB
AETLQFIDSS	MYB-NFIB
SLRICDWTM	MYB-NFIB / MYBL1-NFIB
MQLRICDWTM	MYBL1-NFIB
ISDMQSWYL	MYBL1-NFIB
DMQSWYLG	MYBL1-NFIB
IVLRICDWTM	MYBL1-NFIB
VLRICDWTM	MYBL1-NFIB
KRIPSSWYL	MYBL1-NFIB
MMYSPICLTQT	NFIB-MYB
YSPICLTQFL	NFIB-MYB
FLHQQQFL	NFIB-MYB
FLHQQQFLNT	NFIB-MYB
ASPTATILK	NFIB-MYB
EAASPTATILK	NFIB-MYB
GEAASPTATI	NFIB-MYB
EAASPTATI	NFIB-MYB
SPQTSQFL	NFIB-MYB
SSPQTSQFL	NFIB-MYB

Supplementary Table 9 – Primer sequences for cloning MYB-NFIB / NFIB-MYB fusions. The cloning strategy is shown with the appropriate primer pairs.

Primer name	Sequence	Comments	Template
MYB-N-term			
MYB-1F	CACACA-CGTCTC-GAATTC-ATGGCCCGAAGACCCCGGCACAG	PCR with MYB-1F + MYB-6R, digest with BsmBI	ACC_M9 cDNA (from fresh frozen tumor RNA)
MYB-6R	CACACA-CGTCTC-GGATCC-AGAATCTATAAATTGGAGTGTT		
MYB-NFIB Fusion 1			
MYB-1F	CACACA-CGTCTC-GAATTC-ATGGCCCGAAGACCCCGGCACAG	PCR with MYB-1F + MYB-3R, digest with BsmBI	ACC_M9 cDNA (from fresh frozen tumor RNA)
MYB-3R	TGTGTG-CGTCTCA-AGAATCTATAAATTGGAGTGTT		
NFIB-4F	CACACA-CGTCTCA-TTCTCTGAGGATTTGTGACTGG	PCR with NFIB-4F + NFIB-2R, digest with BamHI	ACC_M9 cDNA (from fresh frozen tumor RNA)
NFIB-2R	TGTGTG-GGATCC-GTTGCTTGTTTCTGCTTGAAGG		
MYB-NFIB Fusion 2			
MYB-1F	CACACA-CGTCTC-GAATTC-ATGGCCCGAAGACCCCGGCACAG	PCR with MYB-1F + MYB-8R, digest with BsmBI	ACC_M9 cDNA (from fresh frozen tumor RNA)
MYB-8R	CACACA-CGTCTC-GGATCC-GCCCAGGTACCAGGA-AGAATCTATAAATTGGAGTGTT		
MYB-NFIB Fusion 3			
MYB-1F	CACACA-CGTCTC-GAATTC-ATGGCCCGAAGACCCCGGCACAG	PCR with MYB-1F + MYB-2R, digest with BsmBI	ACC_M9 cDNA (from fresh frozen tumor RNA)
MYB-2R	TGTGTG-CGTCTCA-TCAG-CTGCGAGGGAGAGAAGGGTAG		
NFIB-3F	CACACA-CGTCTCA-CTGAGGATTTGTGACTGGACC	PCR with NFIB-3F + NFIB-2R, digest with BamHI	ACC_M9 cDNA (from fresh frozen tumor RNA)
NFIB-2R	TGTGTG-GGATCC-GTTGCTTGTTTCTGCTTGAAGG		
NFIB-MYB Fusion 7			
NFIB-6F	CACACA-CGTCTC-GAATTC-ATGATGTATTCTCCCATCTGTCTCACTCAG-ACACAGAACCACACATGCAGCTAC	PCR with NFIB-6F + MYB-1R, digest with BsmBI	ACC_M12 cDNA (from fresh frozen tumor RNA)
MYB-1R	TGTGTG-CGTCTC-GGATCC-CATGACCAGCGTCCGGGCTGAGA		
MYB-NFIB Fusion 8			
MYB-1F	CACACA-CGTCTC-GAATTC-ATGGCCCGAAGACCCCGGCACAG	PCR with MYB-1F + NFIB-6R, digest with BsmBI	ACC_M12 cDNA (from fresh frozen tumor RNA)
NFIB-6R	CACACA-CGTCTC-GGATCC-GCCCAGGTACCAGGACTGCAAGGGGCTCGC		
MYB-NFIB Fusion 9			
MYB-1F	CACACA-CGTCTC-GAATTC-ATGGCCCGAAGACCCCGGCACAG	PCR with MYB-1F + NFIB-7R, digest with BsmBI	ACC_M12 cDNA (from fresh frozen tumor RNA)
NFIB-7R	CACACA-CGTCTC-GGATCC-GTCCCACATATCGATTGGCTTGAGATGTGCCTGAGGCTGTGTAGG-CTGCAAGGGGCTCGC		